# Turning Rubber into a Glass: Mechanical Reinforcement by Nano-Phase Separation.

Martin Tress<sup>1\*†</sup>, Sirui Ge<sup>2</sup>, Kunyue Xing<sup>1</sup>, Peng-Fei Cao<sup>3</sup>, Tomonori Saito<sup>3</sup>, Anne-Caroline Genix<sup>4</sup> and Alexei P. Sokolov<sup>1,3\*</sup>

<sup>1</sup>University of Tennessee, Knoxville, Department of Chemistry, Knoxville, Tennessee 37996, United States <sup>2</sup>University of Tennessee, Knoxville, Department of Materials Science, Knoxville, Tennessee 37996, United States <sup>3</sup>Oak Ridge National Laboratory, Chemical Sciences Division, Oak Ridge, Tennessee 37831, United States <sup>4</sup>Laboratoire Charles Coulomb (L2C), Université de Montpellier, CNRS, F-34095 Montpellier, France *Keywords: associating polymer, supramolecular bond, mechanical reinforcement, phase separation, interfacial layer.* 

**ABSTRACT:** Supramolecular associations provide a promising route to functional materials with properties such as self-healing, easy recyclability or extraordinary mechanical strength and toughness. The latter benefit especially from the transient character of the formed network, which enables dissipation of energy as well as regeneration of the internal structures. However, recent investigations revealed intrinsic limitations in the achievable mechanical enhancement. This manuscript presents studies of a set of telechelic polymers with hydrogen-bonding chain ends exhibiting an extraordinarily high, almost glass-like rubbery plateau. This is ascribed to segregation of the associative ends into clusters and formation of an interfacial layer surrounding these clusters. An approach adopted from the field of polymer nanocomposites provides a quantitative description of the data and reveals strongly altered mechanical properties of the polymer in the interfacial layer. These results demonstrate how employing phase separating dynamic bonds can lead to the creation of high-performance materials.

Supramolecular association is a thriving concept to develop novel functional and responsive materials.<sup>[1-8]</sup> Mimicking many examples from nature,<sup>[9-12]</sup> hierarchical super-structures formed by transient networks give rise to highly desirable properties such as self-healing, [3-6] super-stretchability, [2] mechanical enhancement, [13] recyclability, [14-16] etc. [7,8] In order to fully incorporate this concept into technology and materials design, it is crucial to understand the details of the association process on the molecular scale and the relations to the resulting macroscopic properties. An analysis of linear polymers with hydrogen-bonding end groups demonstrated that the Bond Lifetime Renormalization Model (BLRM)<sup>[17]</sup> can quantitatively describe the relation between molecular associations and macroscopic network relaxation.[18,19] This enables one to predict material performance based on its chemical structure, i.e. it provides a big step towards rational design of functional materials. The model also reveals intrinsic limitations in the network stability, namely a tradeoff between a high rubbery plateau modulus and long network relaxation time; increasing one of these two parameters will automatically reduce the other. [20] However, there are indications that this limit might be overcome by a particular choice of H-bonding end groups which phase separate from the main chains; [20,21] but rarely rubbery plateaus exceeding the range of ~10 MPa and extending over more than 15 decades in frequency are reported.[J. Am. Chem. Soc. 2010, 132, 34, 12051–12058 Moreover, the underlying type of heterogeneous structure is not captured by the BLRM and thus requires a different theoretical approach. While the aggregation of such functional end groups in multiplet clusters and a resulting enhancement of the mechanical properties is well established, certain

aspects of the dynamics are yet to be explored. [Macromolecules 2017, 50, 2973–2985 {4}] Although efforts have been taken to understand the connection between the structural relaxation rate and macroscopic flow rates, [Scientific Reports | 6:32356 {5}] the design of a maximized rubbery plateau modulus is not yet understood.

Here, we present a set of telechelic polymers with H-bonding end groups which combine an extremely high shear modulus plateau (of almost glass-like value ~100 MPa) with dramatically prolonged network relaxation time. This extraordinary mechanical enhancement bears a striking similarity to polymer nanocomposite materials, and an approach adopted from that field unravels the molecular origin of the reinforcement which by far exceeds a hard-filler-effect of the segregated glassy end group clusters. We ascribe this tremendous reinforcement to a severe alteration of chain conformation and mobility in the interfacial polymer region around these clusters.

The complex shear modulus master curves (created using time-temperature-superposition with horizontal shifts only) of polydimethylsiloxane (PDMS) based linear telechelic polymers with different degree of polymerization (DP), all terminated with 4-(propylamino)-4-oxobutanoic acid (POA) groups (chemical structure Figure 1a, for synthesis see SI), exhibits features characteristic for rather long polymers (Figure 1b): (i) a glassy regime at high frequency with a step in the real part G' reaching up to  $\sim$ 1 GPa and at the same position the segmental relaxation peak in the loss part G''; (ii) an extended rubbery plateau in G' at intermediate frequencies; and (iii) the terminal re-

laxation (end of the plateau) at low frequencies, usually ascribed to the longest chain relaxation time in simple (non-associating) polymers. In simple systems, the terminal relaxation time strongly increases with chain length. Hence, the observed separation of  $\sim$ 10-15 orders of magnitude between segmental and terminal relaxation time (Figure 1) would usually occur in polymers with DP above  $10^4$ . The studied systems, however, have much shorter chains (DP = 13-74); thus, the long rubbery plateau clearly reflects the mechanical reinforcement due to the

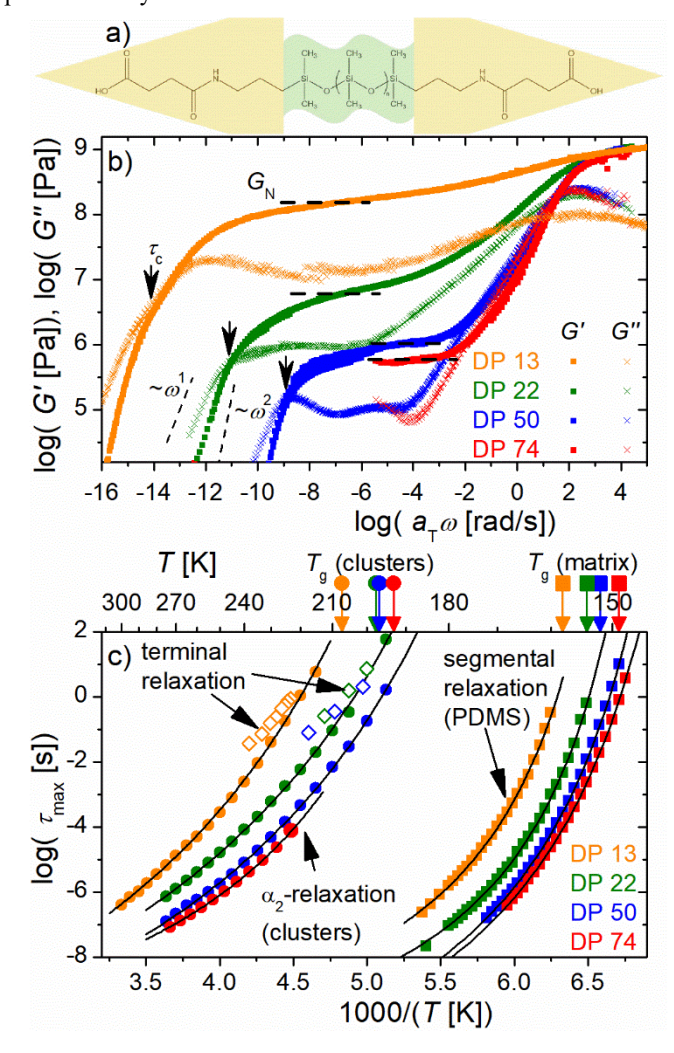


Figure 1. a) Chemical structure of the supramolecular polymers; the polydimethylsiloxane (PDMS) main chain and 4-(propylamino)-4oxobutanoic acid ends are highlighted green and yellow, respectively. b) Master curves of the storage G' (closed symbols) and loss G'' (open symbols) part of the shear modulus, respectively, of these polymers with different degree of polymerization (DP), as indicated. The plateau modulus  $G_N$  and the terminal relaxation time  $\tau c$ are indicated by horizontal dashed lines and vertical arrows, respectively, c) Activation plot showing the characteristic times of several relaxation processes deduced from broadband dielectric spectroscopy (closed symbols) and small amplitude oscillatory shear rheology (open symbols) as labeled. The vertical arrows marked with squares and circles depict the calorimetric glass transitions of the PDMS matrix and the end group clusters, respectively. The extraordinary enhancement of the rubbery plateau and its unexpected dependence on MW of the main chain are strong indicators for an

supramolecular bonds, and the terminal relaxation indicates stress release from the transient network. Furthermore, with decreasing DP, both the rubbery plateau modulus as well as the terminal relaxation time increase; opposing the results of earlier studies on H-bonding telechelic polymers and the prediction of the lifetime renormalization model.<sup>[17,19,20]</sup> For the shortest chain with DP = 13, the plateau modulus has a value above 100 MPa, being closer to a glassy modulus than to the rubbery plateau in entangled PDMS (< 0.5 MPa).<sup>[22]</sup>

unusual effect not seen in most other associating polymers. Differential scanning calorimetry (DSC) reveals a second glass transition process ~50-60 K above the  $T_{\rm g}$  of the PDMS main chain (Figure S1), clearly indicating a phase separation. Additionally, broadband dielectric spectroscopy (BDS) shows a slow relaxation process in these materials (Figure S2) which reaches a relaxation time  $\tau_{\alpha 2}$  of ~100 s at the second  $T_{\rm g}$  (Figure 1b). Its relaxation strength scales linearly with the fraction of the end groups. [21] Thus, the BDS data provide clear evidence that the second  $T_{\rm g}$  is related to the phase separated end groups forming glassy clusters at lower temperatures.

More evidence of the phase separation comes from X-ray scattering which shows a pronounced peak at a relatively small wave vector  $q_{\text{max}}$  (Figure 2a) which is not present in unmodified PDMS or in PDMS with non-phase separating H-bonding end groups. Since this peak is present at room temperature (Fig. 2a), any type of self-assembly-transition is ruled out in the studied temperature range. The peak position provides a rough estimate of the average center-to-center distance between clusters,  $\langle d \rangle \approx 2\pi \ q_{\rm max}^{-1}$  corresponding to ~4 - 5.7 nm. With decreasing main chain length, the peak intensity increases and its position shifts to higher q. The former reflects the increasing volume fraction of the clusters while the latter indicates a reduction in inter-cluster distance (Figure 2a). Assuming that a majority of chain ends segregate to these clusters and using the weight fraction of the end groups (and assuming the difference in mass densities to be negligible), the average size of the clusters is estimated to be  $\langle R \rangle = 1.2 - 1.4$  nm (Figure 2b), and the corresponding number of chain ends per cluster is ~30-50 (Figure 2c).

An increase in shear modulus caused by chains extended beyond their unperturbed conformation is well-known, and can be accounted for by a pre-factor to the classical rubber elasticity estimate equal to the squared ratio of the actual (stretched)  $\langle \tilde{R}_{ee} \rangle$ in the network to its unperturbed value  $R_{ee}$  [24,25]. An estimate of this effect using  $\langle \tilde{R}_{ee} \rangle = \langle d \rangle - \langle R \rangle$  from the X-ray measurements (see SI for details of this and other model estimates) predicts only a small increase by a factor of less than 3 (Figure 3a). An additional enhancement of the modulus arises from the hard glassy clusters in the soft polymeric matrix and its magnitude can be estimated using a classical two-phase model (TPM) which yields the shear modulus of a composite system of a matrix with dispersed filler particles. [26-29] The parameters are shear moduli and Poisson ratios of both phases and their volume ratio. The latter is approximated with the weight fraction of end groups (i.e. assuming comparable density to the matrix). For the matrix modulus, the classical entangled rubber modulus is used and Poisson's ratio of crosslinked PDMS ( $\sigma_m = 0.495$ ) is taken from literature. [30] For the clusters,  $G_f = 3 \times 10^9$  Pa, typical for glassy systems, and  $\sigma_f = 0.33$ , typical for H-bonding liquids like glycerol, are assumed.<sup>[31]</sup> This (see SI for details) still vastly underestimates the experimental results, even if combined with the mentioned approximation of chain stretching (Figure 3a).

The striking structural similarity of the studied systems to polymer nanocomposites (PNCs) Rub. Chem. Tech. 45, 1171 (1972){1}; 46, 877 (1973) {2}; 51, 437 (1978) {3}] suggests that the mechanical reinforcement might also have a similar origin. Several PNC studies have established the existence of an interfacial polymer layer around the filler particles with strongly altered properties. [32-34] This concept was proposed for elastomers with ionic clusters already in 1990.[35] The interfacial layer model (ILM) that accounts for the combined contributions of the nanoparticles, the neat matrix, and the enhanced modulus of the interfacial layer provides a proper description of the shear modulus in PNCs. [33] This model, using the parameters from the TPM complemented by shear modulus and Poisson ratio of the interfacial layer and its volume fraction (see SI for details), can also describe the enhanced moduli observed in the presented associating polymers (Figure 3a), which suggests the presence of an interfacial layer and remarkable changes of the mechanical properties therein. First of all, to match the ILM to the experimental data, the interfacial layer has to be assumed to have a glass-like shear modulus ( $G_1 = 10^9 \text{ Pa}$ ,  $\sigma_1 = 0.495$ ). This may be understood by steric hindrance of the chains protruding from the clusters. These end group aggregates correspond to grafted ("hairy") nanoparticles with a quite high grafting density of  $\sim 1.6 - 2$  chains per nm<sup>2</sup> (considerably higher than the ~0.3 chains per nm<sup>2</sup> usually found in grafted nanoparticles).<sup>[36]</sup> It means that chains in the interfacial layer will be strongly stretched (Figure 3c), likely causing the high shear modulus.

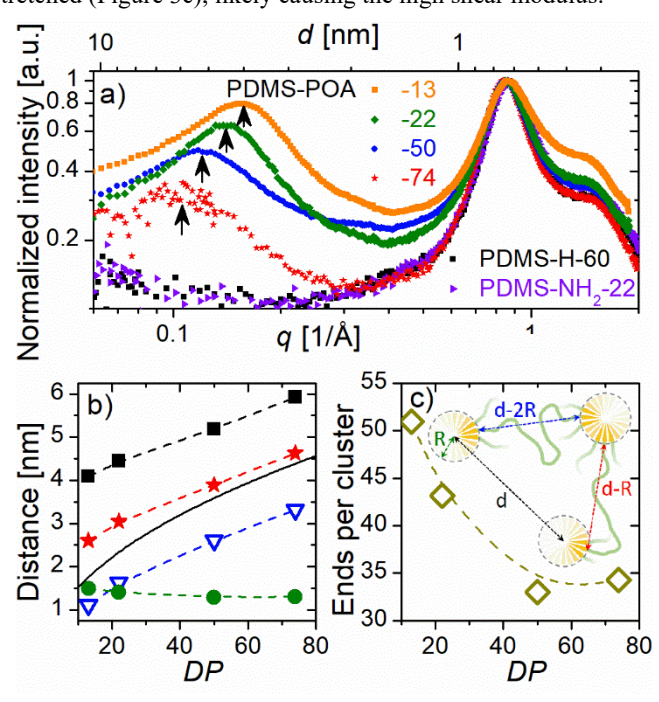


Figure 2. a) Wave-vector q dependence of the X-ray scattering intensity of telechelic polydimethylsiloxane terminated with 4-(propylamino)-4-oxobutanoic acid (PDMS-POA) with different degree of polymerization (DP) as indicated measured at room temperature. As references, we also present the data of a non-associating PDMS with DP = 60 (PDMS-H-60) and a 3-aminopropyl terminated PDMS without phase separation and DP = 22 (PDMS-NH<sub>2</sub>-22). The vertical arrows indicate the peak assigned to the scattering from end group clusters for the phase separating systems. b) Average distance between these clusters  $\langle d \rangle$  deduced from the X-ray

peaks (solid black squares), average cluster radius  $\langle R \rangle$  estimated from  $\langle d \rangle$  and the volume fraction of the end groups (solid green circles) and different inter-cluster distances  $\langle d \rangle$ -2 $\langle R \rangle$  (open blue triangles) and  $\langle d \rangle - \langle R \rangle$  (solid red stars) compared to the calculated endto-end vector Ree of the unperturbed main chain (solid line). c) Average number of end groups per cluster. The inset sketches the different distances presented in panel b). The dashed lines in panel b) and c) are guides to the eye. To understand the greatly enhanced mechanical properties of the studied systems, we start from classical rubber elasticity estimates, where the shear modulus is defined by the molecular weight between crosslinks. [23] This approach (see SI for details) clearly underestimates the plateau level, and the difference to the experimental data increases with decreasing chain length, reaching a factor of  $\sim$ 100 for the sample with DP = 13 (Figure 3a). To reveal a potential role of chain stretching, we analyze the relationship between inter-clusters distance and end-to-end distance of unperturbed chains  $R_{ee}$ . The shortest average separation between the surfaces of adjacent clusters is  $\langle d \rangle$ -2 $\langle R \rangle$  (inset Figure 2c). However, many chains are expected to connect the faces of the clusters on longer paths. For simplicity, we approximate the average end-to-end length of a connecting chain by  $\langle d \rangle - \langle R \rangle$  (inset Figure 2c). For the longer chains (DP = 74), the estimated  $\langle d \rangle - \langle R \rangle$  indeed agrees well with the unperturbed  $R_{ee}$  of the chain. In contrast, for the shorter chains,  $R_{ee}$  is much smaller than  $\langle d \rangle - \langle R \rangle$ , up to a factor of 1.4 at DP = 13 (Figure 2b). This suggests a significant stretching for the majority of the chains in the systems with low *DP*.

Using the ILM, a proper description of the experimental data is achieved (Figure 3a) by assuming a volume of the interfacial layer which corresponds to a thickness of ~0.6 - 0.7 nm (the volume of this layer corresponds to 4-6 repeat units per chain). This is much thinner than the interfacial layer observed in PNCs (~3-5 nm), [32-34] which is consistent with much smaller radius of the clusters. Moreover, due to the small size of the clusters and the short distance between them, this relatively thin layer still comprises of about 90% of the main chain segments in the case of the shortest studied polymer, causing the overall shear modulus to raise up by a factor of almost 100. We emphasize that these are rough estimates since a potential percolating network formed by the interfacial regions is most likely present in the sample with DP = 13. Nevertheless, the proposed approach provides a clear semi-quantitative description of the observed increase of the rubbery plateau modulus.

The crucial impact of the chain end aggregation is also obvious in the tremendous increase of zero shear viscosity (Figure 3b). Scaling with  $T_{\rm g}$  of the main chain polymer roughly collapses the viscosities of several telechelic PDMS of similar length with various H-bonding end groups which do not phase separate. However, despite this scaling, the viscosity of POA terminated systems exceeds the other ones by several decades (Figure 3b). Surprisingly, scaling with the  $T_{\rm g}$  of the end group clusters yields curves close to the viscosity in systems without phase separation (Figure 3b). This emphasizes the critical role of the  $T_{\rm g}$  of the clusters in the viscoelastic properties of associating polymers with phase separation, which is usually not considered in current models. While related to vitrimers the absence of phase separation there is a significant difference; their viscosity relies on switching of individual dynamic bonds.

The presented systems demonstrate that employing phase separation of functional groups as association mechanism in polymers can create materials that combine unique properties

П

of supramolecular substances (stretchability, self-healing, processability, recyclability) with the mechanical strength of nanocomposites. The achieved tremendous enhancement of mechanical properties greatly surpasses usual PNCs. [33] An explanation for such an enhancement is a severe alteration of chain conformations in the interfacial layer surrounding segregated end group clusters, and the very small distance between them. Here, the regular structure of telechelic systems with uniform chain lengths between stickers seems relevant, in contrast to randomly functionalized systems with a distribution of sticker separations and far smaller modulus enhancement. [3] These results demonstrate the great potential of supramolecular reversible bonds combined with phase separation behavior for design of functional recyclable materials with unique properties.

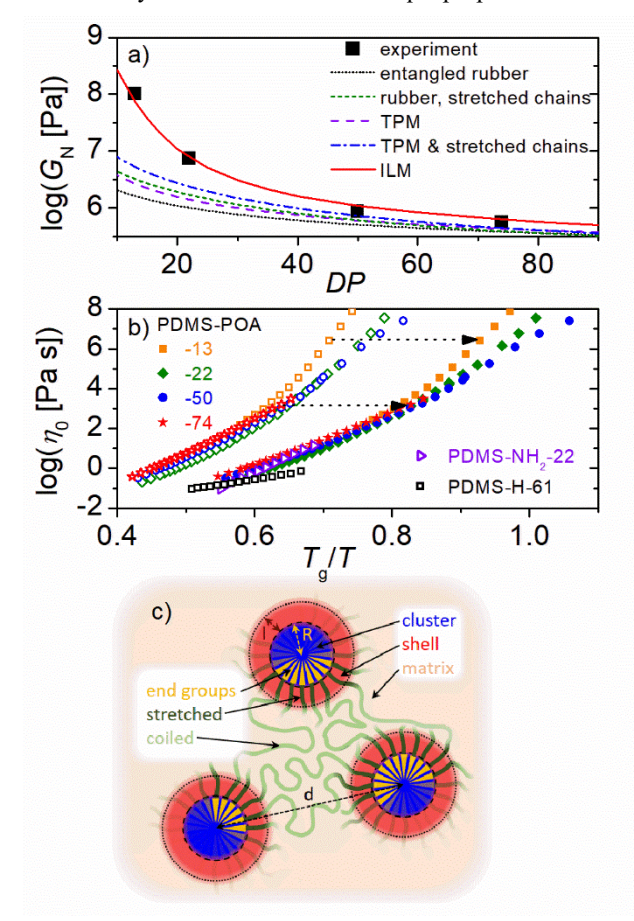


Figure 3. a) Experimentally determined rubbery plateau of the shear modulus of several 4-(propylamino)-4-oxobutanoic acid terminated polydimethylsiloxane (PDMS-POA) vs. DP of the main chain as well as theoretical predictions for a cross linked and entangled rubber (the chain ends are considered to be the cross links), the same cross linked and entangled rubber considering stretched chain conformations<sup>[24,25]</sup> according to inter-cluster separations (deduced by X-ray scattering), a two-layer-model (TPM)[26-29] describing the clusters as hard fillers in a soft polymer matrix, and a numerical approximation by the interfacial-layer-model (ILM)[33] assuming a mechanically enhanced layer around the clusters (see text for details). b) Zero shear viscosity  $\eta_0$  vs. inverse temperature scaled by Tg of the PDMS matrix for different end groups of telechelic chains as indicated (open symbols); for PDMS-POA, also scaling with respect to the  $T_{\rm g}$  of the end group clusters is shown (closed symbols). The dashed arrows visualize how the curves shift

when instead of the matrix  $T_{\rm g}$  the cluster  $T_{\rm g}$  is used for scaling. c) Sketch of end group clusters connected by the chains with a stretched portion surrounding the clusters and forming an interfacial layer with high modulus.

## **Experimental Section/Methods**

Synthesis of 4-(propylamino)-4-oxobutanoic acid terminated polydimethylsiloxane (PDMS-NHCO-COOH) is based on a nucleophilic reaction of aminopropyl-terminated PDMS (PDMS-NH<sub>2</sub>) with succinic anhydride. For that, PDMS-NH<sub>2</sub> (5 mmol, used as received from Gelest) and triethylamine (15 mmol, distilled under calcium hydride before use) were dissolved in anhydrous tetrahydrofuran (THF). Then, 4-(dimethylamino)-pyridine (5 mmol) and succinic anhydride (20 mmol) dissolved in anhydrous THF were added to the PDMS-NH2 solution and the mixture is allowed to react at 40°C for 2 days under inert atmosphere. Subsequently, the organic solvent has been evaporated after which hydrochloric acid solution (1 mol/L) was added and stirred for 1 hour. The product was extracted by dichloromethane (DCM) for 3 times, and the solution was dried with anhydrous sodium sulfate. The final product was obtained by drying in a vacuum oven for 3 days. Prior to any of the following characterization methods, the samples were annealed at 313 K for 5 days in vacuum (0.1 mbar) to remove residual solvents and moisture. The structure of synthesized molecules was confirmed by <sup>1</sup>H NMR spectra as shown for related materials in our previous reports.[21]

**Differential Scanning Calorimetry** (DSC) measurements were done with a Q-1000 differential scanning calorimeter (TA Instruments) in aluminum hermetic pans. In two cooling and heating cycles ranging from 140 to 275 K at a rate of 10 K min  $^{\rm l}$  the thermal history was removed and  $T_{\rm g}$  was determined from the midpoint of the corresponding step in heat flow of the second heating using the respective function of the TA Universal Analysis 2000 software.

Small Amplitude Oscillatory Shear (SAOS) rheology was conducted on an AR2000ex (TA instruments) rheometer at angular frequencies ranging from  $10^{-1}$  to  $10^2$  rad s<sup>-1</sup> in the stress-controlled mode. A parallel plate geometry was employed using a disk diameter of 4 and 8 mm depending on the magnitude of the shear modulus and a constant gap of 0.5 mm between the plates. Thermal equilibrium was ensured by temperature stabilization for 10 min, and deviations were set to be smaller than 0.2 K. To guarantee a linear SAOS response, a strain sweep measurement preceded the full scan at each temperature. From these data sets, zero shear viscosities in the range  $\eta_0 > 10^5$  Pa·s were calculated using  $\eta_0 = \lim_{\omega \to 0} G''$   $\omega^{-1}$ . Smaller viscosity values were determined in continuous ramp measurements at a shear rate of 10 rad s<sup>-1</sup> using conical plates of 25 mm diameter with a cone angle of  $2^{\circ}$  and a truncation of 58  $\mu$ m.

**Broadband Dielectric Spectroscopy** (BDS) measurements were recorded with an Alpha-A impedance analyzer connected to a Quatro Cryosystem for temperature control (both from Novocontrol). The samples were loaded in a measurement cell made of invar steel and a sapphire disk with an electrode diameter of 12 mm and a separation of 49  $\mu$ m (empty cell capacitance of ~20 pF); further details of the cell can be found elsewhere. [38] Isothermal spectra were recorded at frequencies ranging from  $10^{-2}$  to  $10^{6}$  Hz at temperatures between 150 and 270 K; each scan was preceded by 10 min of thermal stabilization and no deviation above 0.2 K was allowed.

**X-ray Scattering** experiments were performed with an inhouse setup of the Laboratoire Charles Coulomb, "Réseau X et gamma", Université Montpellier, France. A high brightness low power X-ray tube, coupled with aspheric multilayer optic (GeniX3D from Xenocs) delivered an ultralow divergent beam (0.5 mrad, flux 35 Mphotons s<sup>-1</sup>,  $\lambda = 1.5418$  Å). The scattered intensity was measured by a 2D pixel "Pilatus" detector with a sample-to-detector distance of 20 cm. Samples were prepared in glass capillaries. All intensities were corrected by transmission and the empty cell contribution was subtracted.

### ASSOCIATED CONTENT

**Supporting Information**. Characteristic properties, DSC trace, and dielectric spectra of the studied polymers; description of multicomponent models for shear modulus. This material is available free of charge via the Internet at http://pubs.acs.org

### **AUTHOR INFORMATION**

# Corresponding Author

\*Correspondence to: <a href="martin.tress@uni-leipzig.de">martin.tress@uni-leipzig.de</a>, <a href="martin.tress@uni-leipzig.de">sokolov@utk.edu</a>

### **Present Addresses**

†Present address: Leipzig University, Leipzig, Germany

#### **Author Contributions**

The manuscript was written through contributions of all authors. All authors gave approval to the final version of the manuscript.

### **Funding Sources**

National Science Foundation, Alexander von Humboldt Foundation, United States Department of Energy.

## **ACKNOWLEDGMENT**

This work was supported by the NSF Polymer program under grant DMR-1904657. MT is grateful to the Alexander von Humboldt Foundation for granting him a Feodor-Lynen fellowship. PC and TS acknowledge partial financial support for polymer synthesis by the U.S. Department of Energy, Office of Science, Basic Energy Sciences, Materials Science & Engineering Division.

#### **REFERENCES**

- K. Xing, S. Chatterjee, T. Saito, C. Gainaru, A. P. Sokolov, Impact of hydrogen bonding on dynamics of hydroxyl-terminated polydimethylsiloxane. *Macromolecules* 2016, 49, 3138
- [2] P. F. Cao, B. Li, T. Hong, J. Townsend, Z. Qiang, K. Xing, K. D. Vogiatzis, Y. Wang, J. W. Mays, A. P. Sokolov, Super-stretchable, self-healing polymeric elastomers with tunable properties. Adv. Funct. Mater. 2018, 28, 1800741.
- [3] C. Schubert, P. Dreier, T. Nguyen, K. Maciol, J. Blankenburg, C. Friedrich, H. Frey, Synthesis of linear polyglycerols with tailored degree of methylation by copolymerization and the effect on thermorheological behavior. *Polymer* 2017, 121, 328.
- [4] P. Cordier, F. Tournilhac, C. Soulie-Ziakovic, L. Leibler, Self-healing and thermoreversible rubber from supramolecular assembly. *Nature*, 2008, 451, 977.
- [5] A. Campanella, D. Döhler, W. H. Binder, Self-healing in supramolecular polymers. *Macromol. Rapid Commun.* 2018, 39, 1700739.

- [6] Y.-F. Huang, J.-Z. Xu, J.-Y. Xu, Z.-C. Zhang, B. S. Hsiao, L. Xu, Z.-M. Li, Self-reinforced polyethylene blend for artificial joint application. *J. Mater. Chem. B* 2014, 2, 971.
- [7] J. Li, J.A. Viveros, M.H. Wrue, M. Anthamatten, Shapememory effects in polymer networks containing reversibly associating side-groups. Adv. Mater. 2007, 19, 2851.
- [8] A. Noro, M. Hayashi, Y. Matsushita, Design and properties of supramolecular polymer gels. *Soft Matter* 2012, 8, 6416.
- [9] A. Hagenau M. H. Suhre, T. R. Scheibel, Nature as a blueprint for polymer material concepts: Protein fiber-reinforced composites as holdfasts of mussels. *Prog. Polym. Sci.* 2014, 39, 1564.
- [10] D. S. Fudge, N. Levy, S. Chiu, J. M. Gosline, Composition, morphology and mechanics of hagfish slime. *J. Exp. Biol.* 2005, 208, 4613.
- [11] F. Vollrath, D. Porter, Spider silk as archetypal protein elastomer. *Soft Matter* **2006**, *2*, 377.
- [12] C. Rieu, L. Bertinetti, R. Schuetz, C. C. A. Salinas-Zavala, J. C. Weaver, P. Fratzl, A. Miserez, A. Masic, The role of water on the structure and mechanical properties of a thermoplastic natural block co-polymer from squid sucker ring teeth. *Bioinspir. Biomim.* 2016, 11, 055003.
- [13] E. Filippidi, T.R. Cristiani, C.D. Eisenbach, J.H. Waite, J.N. Israelachvili, B.K. Ahn, M.T. Valentine, Toughening elastomers using mussel-inspired iron-catechol complexes. *Science* 2017, 358, 502.
- [14] B.J.B. Folmer, R.P. Sijbesma, R.M. Versteegen, J.A.J. vander Rijt, E.W. Meijer, Supramolecular polymer materials: chain extension of telechelic polymers using a reactive hydrogen-bonding synthon. *Adv. Mater.* 2000, *12*, 874.
- [15] K.E. Feldman, M.J. Kade, E.W. Meijer, C.J. Hawker, E.J. Kramer, Model transient networks from strongly hydrogenbonded polymers. *Macromolecules* 2009, 42, 9072.
- [16] Z.P. Zhang, M.Z. Rong, M.Q. Zhang, Polymer engineering based on reversible covalent chemistry: A promising innovative pathway towards new materials and new functionalities. *Prog. Polym. Sci.* 2018, 80, 39.
- [17] E. B. Stukalin, L.-H. Cai, N. A. Kumar, L. Leibler, M. Rubinstein, Self-healing of unentangled polymer networks with reversible bonds. *Macromolecules* 2013, 46, 7525.
- [18] B. J. Gold, C. H. Hövelmann, N. Lühmann, N. K. Székely, W. Pyckhout-Hintzen, A. Wischnewski and D. Richter, Importance of compact random walks for the rheology of transient networks. ACS Macro Lett. 2017, 6, 73.
- [19] S. Ge, M. Tress, K. Xing, P. Cao, T. Saito, A. P. Sokolov, Viscoelasticity in associating oligomers and polymers: experimental test of the bond lifetime renormalization model. *Soft Matter* 2020, 16, 390.
- [20] M. Tress, K. Xing, S. Ge, P. Cao, T. Saito, A. Sokolov, What dielectric spectroscopy can tell us about supramolecular networks. *Eur. Phys. J. E* 2019, 42, 133.
- [21] K. Xing, M. Tress, P. Cao, S. Cheng, T. Saito, V. N. Novikov, A. P. Sokolov, Hydrogen-bond strength changes network dynamics in associating telechelic PDMS. *Soft Mat*ter, 2018, 14, 1235.
- [22] C. W. Macosko, G. S. Benjamin, Modulus of three and four functional poly (dimethylsiloxane) networks. *Pure & Appl. Chem.* 1981, 53, 1505.
- [23] M. Rubinstein, R. H. Colby, *Polymer Physics*, Oxford University Press, 2004
- [24] P. J. Flory, A. Ciferri, C. A. J. Hoeve, The thermodynamic analysis of thermoelastic measurements on high elastic materials. *J. Polymer Sci.* 1960, 145, 235.

- [25] D. Katz, A. V. Tobolsky, Rubber elasticity in a highly crosslinked epoxy system. *Polymer* 1963, 4, 417.
- [26] C. van der Poel, On the rheology of concentrated dispersions. *Rheol. Acta* 1958, 1, 198.
- [27] Z. Hashin, S. J. Shtrikman, A variational approach to the theory of the elastic behaviour of multiphase materials. *J. Mech. Phys. Solids* 1963, 11, 127.
- [28] F. H. J. Maurer, in Controlled Interphases in Composite Materials; H. Ishida. Ed., Springer Netherlands 1990; pp 491-504.
- [29] Z. Hashin, Thermoelastic properties of particulate composites with imperfect interface. J. Mech. Phys. Solids 1991, 39, 745.
- [30] A. Müller, M. C. Wapler, U. Wallrabe, A quick and accurate method to determine the Poisson's ratio and the coefficient of thermal expansion of PDMS. Soft Matter 2019, 15, 779.
- [31] A. G. Lyapin, E. L. Gromnitskaya, I. V. Danilov, V. V. Brazhkin, Elastic properties of the hydrogen-bonded liquid and glassy glycerol under high pressure: comparison with propylene carbonate. *RSC Adv.* 2017, 7, 33278.
- [32] A. P. Holt, P. J. Griffin, V. Bocharova, A. L. Agapov, A. E. Imel, M. D. Dadmun, Jo. R. Sangoro, and A. P. Sokolov, Dynamics at the polymer/nanoparticle interface in poly (2-vinylpyridine)/silica nanocomposites. *Macromolecules* 2014, 47, 1837.

- [33] S. Cheng, V. Bocharova, A. Belianinov, S. Xiong, A. Kisliuk, S. Somnath, A. P. Holt, O. S. Ovchinnikova, S. Jesse, H. Martin, T. Etampawala, M. Dadmun, A. P. Sokolov, *Nano Lett.* 2016, 16, 3630.
- [34] S. Cheng, B. Carrol, W. Lu, F. Fan, J.-M. Y. Carrillo, H. Martin, A. P. Holt, N.-G. Kang, V. Bocharova, J. W. Mays, B. G. Sumpter, M. Dadmun, A. P. Sokolov, Unraveling the mechanism of nanoscale mechanical reinforcement in glassy polymer nanocomposites. *Macromolecules* 2017, 50, 2397.
- [35] A. Eisenberg, B. Hird, R. B. Moore, A new multiplet-cluster model for the morphology of random ionomers. *Macromolecules* 1990, 23, 4098.
- [36] A. P. Holt, V. Bocharova, S. Cheng, A. M. Kisliuk, B. T. White, T. Saito, D. Uhrig, J. P. Mahalik, R. Kumar, A. E. Imel, T. Etampawala, H. Martin, N. Sikes, B. G. Sumpter, M. D. Dadmun, A. P. Sokolov, Controlling Interfacial Dynamics: Covalent Bonding versus Physical Adsorption in Polymer Nanocomposites. ACS Nano 2016, 10, 6843.
- [37] H. Fang, W. Ye, Y. Ding, H. H. Winter, Rheology of the critical transition state of an epoxy vitrimer. *Macromolecules* 2020, 53, 4855.
- [38] H. Wagner, R. Richert, Equilibrium and Non-Equilibrium Type β-Relaxations: d-Sorbitol versus o-Terphenyl. *J. Phys. Chem. B* **1999**, *103*, 4071.

